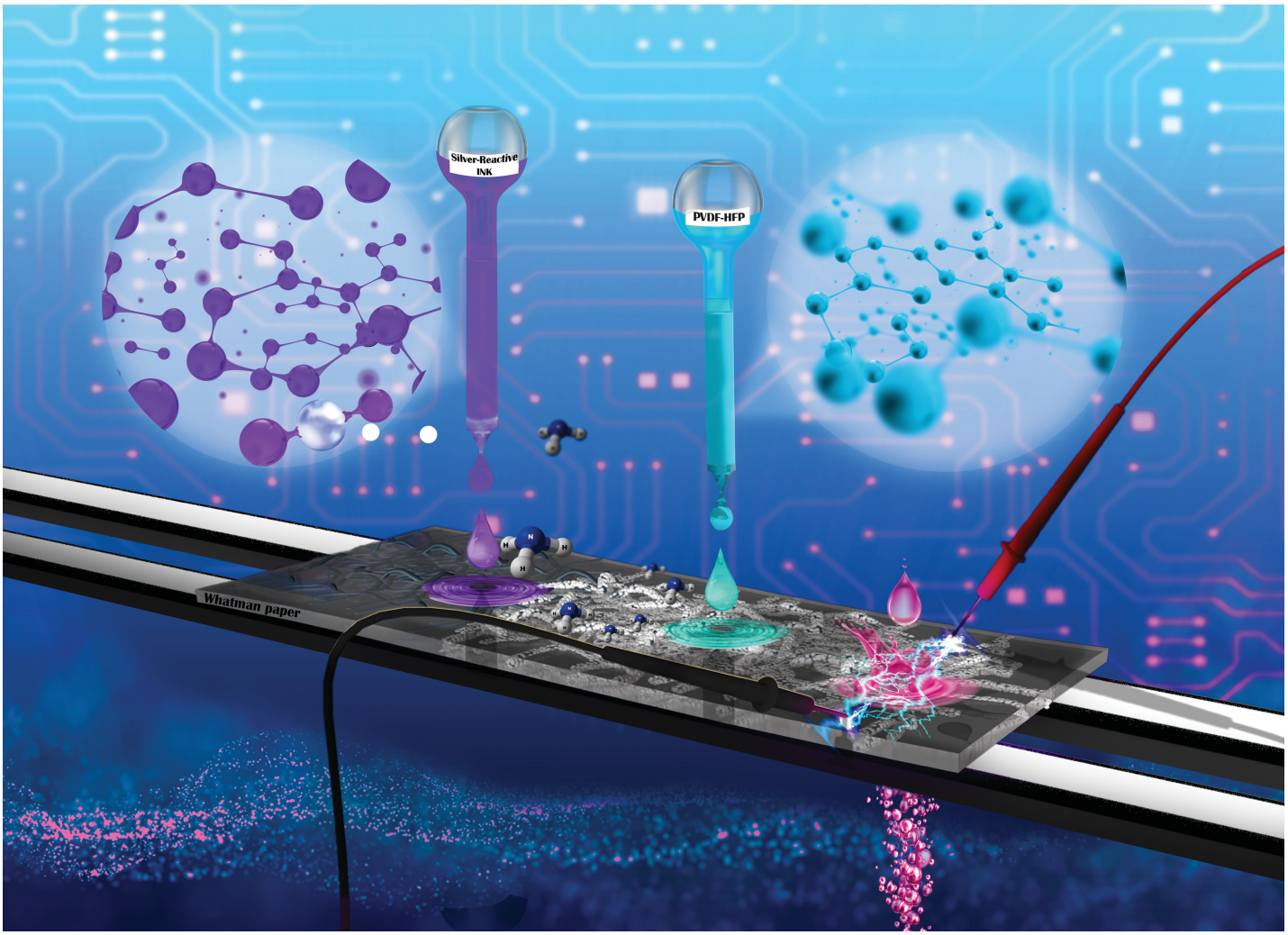

Showcasing research from Professor Yong-Ill Lee's laboratory, Department of Chemistry, Changwon National University, Changwon, Republic of Korea.

Patterning microporous paper with highly conductive silver nanoparticles *via* PVP-modified silver–organic complex ink for development of electric valves

Novel formulation of silver-reactive ink modified by PVP for uniform deposition of highly conductive silver nanoparticles on hydroxyethyl cellulose (HEC)-modified Whatman No. 1 paper was developed and applied as an electric valve for microfluidic device.

As featured in:

See Youngil Lee, Yong-Ill Lee *et al.*, *Mater. Adv.*, 2021, **2**, 3579.

ROYAL SOCIETY OF CHEMISTRY

rsc.li/materials-advances

Registered charity number: 207890

Materials Advances

ROYAL SOCIETY OF CHEMISTRY

PAPER

View Article Online
View Journal | View Issue

Cite this: *Mater. Adv.*, 2021, 2, 3579

Patterning microporous paper with highly conductive silver nanoparticles *via* PVP-modified silver–organic complex ink for development of electric valves†

Mirkomil Sharipov, [ab] Youngil Lee, *[b] Jinsol Han[a] and Yong-Ill Lee *[a]

Received 7th December 2020,
Accepted 14th April 2021

DOI: 10.1039/d0ma00960a

rsc.li/materials-advances

The reactive ink composed of a silver-organic complex has shown potential for developing conductive patterns on various substrates such as glass and PET. However, the incompatibility with Whatman No. 1 and conventional office paper, on which it transduces to silver oxides, has limited its application in developing flexible paper-based electronic devices such as electrofluidics and microfluidics electroanalytical devices. Herein, the stabilization of silver cations generated from silver-reactive ink by polyvinylpyrrolidone (PVP) on hydroxyethyl cellulose (HEC)-premodified Whatman No. 1 paper to induce the formation of silver metal nanoparticles is reported. FTIR studies confirmed the stabilization of silver cations by PVP through nitrogen and oxygen atoms. The modification of paper with HEC prevents the formation of silver oxide and silver acetate salts, thus lowering the curing temperature to 60 °C and achieving high conductivity, calculated to be 6.246×10^6 S m^{-1}. FE-SEM images confirmed the uniform formation of silver nanoparticles on the surface of the cellulose fibers simultaneously preserving the porosity of paper. The microporous silver patterned paper was further coated with a ferroelectric fluoropolymer: PVDF-HFP to enhance its electrowetting properties and was applied in the development of a paper-based microfluidic device equipped with an electrical valve.

1. Introduction

In recent years, the use of inkjet technology to print conductive patterns of significant complexity has received tremendous attention because of its excellent performance when used in the form of a non-contact, digital, and maskless direct deposition.[1] Moreover, this technology is affordable, economical in terms of material consumption, and is scalable for large-scale manufacturing. Inkjet technology has been successfully applied in the development of various electronic devices such as photovoltaic cells,[2] quantum dot light-emitting diodes (QLEDs),[3] organic thin-film transistors,[4] radio-frequency identification devices (RFIDs),[5] and smart clothing.[6]

Two key factors that directly affect the properties of inkjet-printed conductive patterns are the choice of substrate and conductive materials. Thus far, various classes of conductive materials prepared using different methods and substrates have been reported. Ideally, substrates should have a low surface roughness and low permeability to enable the deposition of a thin layer of conductive materials. In this regard, metallic materials have superior conductivity ranging from 10^4 to 10^5 S cm^{-1}. Although alternative conductive materials based on polymers,[7] carbon,[8] graphene,[9] and hybrid nanomaterials[10] are comparatively inexpensive, their conductivities are in the range of 10–10^2 S cm^{-1}, which is two to four orders of magnitude lower than that of metals. The most common methods to prepare patterns based on metallic materials involve the use of inkjet printing to deposit the metal precursors,[11] metal NPs,[12] and organo-metallic compounds.[13] Several papers have reported the preparation of colloidal systems of metallic nanoparticles with small sizes and narrow distribution ranges *via* various methods and their successful application in inkjet printing technology. A few of these methods have yielded good conductivity after a post-treatment process, *i.e.*, sintering at temperatures exceeding 200 °C, which is inappropriate for a paper substrate.[14] Despite the fact that the sintering temperature was lowered to mild temperatures by variation of the coating agent and modifying the preparation methods in recently reported studies, the process of preparing silver NPs remains complicated and requires additional steps. Moreover, in several reported studies silver NPs were synthesized from silver nitrate as the silver precursor, which has the ability to form explosive silver fulminate or silver azide.

[a] *Department of Materials Convergence and System Engineering, Changwon National University, Changwon 51140, Republic of Korea. E-mail: yilee@changwon.ac.kr*
[b] *Department of Chemistry, University of Ulsan, Ulsan 44776, Republic of Korea. E-mail: nmryil@ulsan.ac.kr*

† Electronic supplementary information (ESI) available. See DOI: 10.1039/d0ma00960a

On the other hand, intensive research on organo-metallic compounds led to the development of water-based inks, in which silver is present as a metal–organic complex, also known as reactive inks.[11,15] These types of complexes have a unique property in that they can thermally decompose and release the volatile organic components, thereby resulting in the formation of silver cations, which are further reduced to silver metal NPs. This method stands out among the others because of its simplicity, stability, and low cost compared to methods that require pre-prepared silver NPs. The process to prepare reactive ink is simple and does not require additional steps. Reactive inks possess a good shelf-life, in contrast to the colloidal system, which usually is adversely affected by sedimentation and the agglomeration of NPs. Moreover, the content of the silver component in the silver-reactive ink can exceed 20 wt%, which is larger than the acceptable concentration of metal in the colloidal system. These advantages overcome problems that are often encountered during the inkjet printing process of a colloidal system such as clogging of the head nozzles.

The disadvantage of silver-reactive ink is that it is difficult to apply to any substrate. This type of ink generates silver cations which are effectively reduced to the metallic silver nanoparticles on glass, PET, and PI substrates. Several works reported the deposition of conductive silver tracks on tracing and glossy paper substrate using silver-reactive ink for the development of electronic devices.[16–18] As mentioned by Yang *et al.* sulfuric paper has low permeability, low surface roughness, and good heat resistance that allows post-treatment at 200 °C, making them a good candidate for deposition of conductive silver tracks.[18] However, the low permeability of such substrate renders them unfit for the development of microfluidic devices.

Recently, the development of fully automated and controlled microfluidic devices *via* the integration of stimuli-controlled valves has become popular. The actuation of valves can be controlled by different stimulations such as electric plasma,[19] electrical signal,[20] temperature,[21] liquid,[22] and light.[23] Among various valves, those actuated by the electrical signals are the most convenient and are less sensitive to environmental factors such as light and temperature. Therefore, the ability to print conductive patterns on a conventional and chromatography paper substrate not only holds promise for application in the development of low-cost paper-based microfluidic electroanalytical sensors but is also important in the development of electrical valves.

Based on recent discoveries and the problems that have been encountered in patterning microporous paper with silver nanoparticles using silver organic complex ink, we hypothesized that the hydroxyl groups of cellulose form complexes with silver cations, thereby inducing the formation of nonconductive silver oxide or reversion to salts. To overcome this issue, the integration of a silver cation stabilizing agent in silver-reactive ink has been investigated. Among different stabilizing agents, PVP has been widely studied in the preparation of silver nanoparticles. As reported by Wang *et al.*, PVP acts as a good dispersant and stabilizing agent during the preparation of silver nanoparticles by coordinating with the silver cations *via* its nitrogen and oxygen atoms.[24] However, so far, the integration of PVP in the formula of metal–organic complex ink was not investigated. To the best of our knowledge, we report for the first time the deposition of highly conductive silver patterns on microporous Whatman No. 1 paper substrate *via* the novel formulation of reactive ink based on a silver–organic complex and polyvinylpyrrolidone (PVP). At first, we investigated the stabilizing effect of PVP on silver cations during the decomposition of silver–organic complex and their transformation into silver NPs. Afterward, we studied the effect of modifying the filter paper with HEC on the distribution and curing temperatures of silver NPs. Finally, we coated silver patterns with ferroelectric fluoropolymer poly(vinylidene fluoride-*co*-hexafluoropropylene) (PVDF-HFP) film to enhance their electrowetting properties for application in microfluidic paper-based analytical devices (μPAD) as electro-responsive valves.

2. Experimental section/methods

2.1. Materials

Silver acetate (anhydrous, 99%) was purchased from Alfa-Aesar (South Korea). Polyvinylpyrrolidone powder, average $M_w \sim$ 55 000 was obtained from Sigma-Aldrich (South Korea). Formic acid extra pure reagent, hydroxyethylcellulose 200–400 mPa S, and ammonium hydroxide (28–30%) were purchased from Deajung Chemicals (South Korea). Deionized water was used throughout all the experiments. All chemical reagents were used directly without further purification. Whatman chromatography paper 1 CHR was purchased from GE healthcare life Sciences (USA).

2.2. Characterization

FTIR measurements were performed on a Jasco FT/IR 6300 spectrometer using a diamond ATR crystal. Inks were deposited on wax patterned (1 cm × 1 cm) on Whatman No. 1 paper, dried at room temperature, and annealed at a specific temperature. X-ray diffraction (XRD) was carried out on a Bruker D8 Discover diffractometer with Cu Kα radiation (λ = 0.1542 nm). Inks were deposited on Whatman No. 1 paper (1 cm × 1 cm), dried at room temperature, and annealed at a specific temperature. Samples were fixed to a glass substrate and analyzed. Thermogravimetric analysis (TGA) of the liquid ink was performed using an SDT Q600 V20.9 Build 20 from TA instruments. The prepared liquid ink (100 μL) was deposited in an alumina cup and heated at a rate of 15 °C min^{-1} under nitrogen. Scanning electron microscopy (SEM) was conducted by using a CZ/MIRA I LMH FE-SEM microscope to acquire images of the surface of the silver patterns on the paper substrate. The resistance of the track was measured by using a conventional multimeter using the two-probe method.

2.3. Design of patterns

Patterns were designed on Adobe Illustrator as vectors and printed at the highest resolution. Wax patterns were printed using a Xerox colorqube 8570 printer and heated for 30 seconds at 150 °C to ensure rapid and thorough penetration of the wax.

2.4. Paper modification using HEC

Paper substrates were pre-modified by HEC *via* the drop-cast method. An HEC solution (2 wt%) was prepared by dissolution of 0.2 g of HEC 200–400 mPa S in 10 g of water : MeOH (50 : 50) solution under vigorous stirring at 40 °C. The prepared HEC solution was drop-casted onto the wax patterned paper.

2.5. Preparation of silver–organic complex

The silver acetate diamine complex was prepared by a method that was described previously.[11] Briefly, silver acetate (1 g) was dissolved in 2.5 ml ammonia solution (28–30%) and after stirring for 15 minutes formic acid (200 μL) was added and stirred for another 15 minutes. Separately, 1 g PVP (M_w = 55 000) was added in 6 mL D.I. water and stirred for 30 minutes to completely homogenize the mixture. Afterward, the solution of silver–organic complex, solution of PVP, and DI water were mixed in a ratio of $4 : x : 2 - x$ (where $x \leq 1$) and vortexed for 5 minutes. The PVP stabilized formed complex solution was then filtered through a 0.2 μm membrane filter to remove the formed silver nanoparticles.

2.6. Preparation of silver patterns

The prepared ink was then deposited on different paper substrates, *i.e.*, standard A4 paper, Whatman No. 1 paper, and tracing paper, by using the drop-cast method. Briefly, 50 μL of ink was deposited on the area containing the wax pattern (4 cm × 0.2 cm) and allowed to dry at room temperature for 1 hour.

Upon drying, the formed silver nanoparticles were cured in the oven. The dried paper substrate was placed in the preheated oven at various temperatures (60 °C, 90 °C, and 180 °C) and maintained at these respective temperatures for 3 hours, and 3 hours and 30 minutes, respectively.

2.7. Deposition of PVDF and PVDF-HFP films

The PVDF-HFP solution was prepared by dissolution of PVDF-HFP (M_w ~400 000, ~130 000) in acetone. Briefly, 1 g PVDF-HFP pellets were mixed with 10 g acetone and stirred vigorously for 1 hour at rt. Upon complete dissolution of PVDF-HFP, the solution was applied on silver patterns *via* two methods: dip-coating and drop-casting.

2.8. Fabrication of stacked system

To ensure good contact between silver tracks and paper substrate, a stacked system has been designed. Several approaches to the design system have been reported, including lamination and plastic holders. Several layers of paper were stacked to each other through parafilm and hot-pressed at 100 °C to melt and penetrate parafilm into wax patterns.

3. Results and discussion

3.1. Characterization of PVP-stabilized silver-reactive ink

To study the stabilizing effect of PVP on the silver cations during the decomposition process of reactive ink on a paper substrate we prepared ink modified by various concentrations of PVP, which was drop-casted onto Whatman No. 1 and HEC@Whatman No. 1 filter paper. The schematic illustration and characterization of conductive patterns are illustrated in Fig. 1 and Fig. S1 (ESI†). The FTIR spectra of the paper on which the PVP and PVP-modified ink, respectively, had been deposited, showed that the resonance peaks of both C–O and C–N were affected, see Fig. S1(A) (ESI†). The appearance of a shoulder at 1661 cm^{-1} indicates the stabilization of the silver nanoparticles (of which the size ranges from 500–1000 nm) by the carbonyl group of the PVP.[24] Additionally, the redshift exhibited by the C–N bands at 1019 cm^{-1} and 1056 cm^{-1} confirms the stabilization of silver nanoparticles of smaller size. The formation of silver oxide, which was induced by the deposition of conventional silver-reactive ink on paper, was confirmed by the FTIR spectra, shown in Fig. S1(B) (ESI†). The resonance peaks that appear at 3162 cm^{-1} and 1050 cm^{-1} on the FTIR spectrum of silver complex ink unmodified by PVP on paper are attributed to the Ag–O–H stretching and O–Ag–O vibration of Ag_2O, respectively. The XRD patterns of the reactive ink unmodified by PVP and deposited on paper showed a diffraction peak at 2θ = 38.74° ascribed to the reflections of Ag(111) after heat treatment, as shown in Fig. 1(B). However, the diffraction peak at 2θ = 34.29° confirms the presence of Ag_2O (JCPDS, file No. 42-0874), which is in agreement with the FTIR results. The broad nature of peaks indicates that silver nanoparticles are smaller in size, but also indicates the presence of residual silver acetate and other silver oxides including Ag_3O (JCPDS, file No. 01-074-0878). Additionally, the diffraction peaks at 2θ = 15°, 2θ = 16.5°, and 2θ = 22.4° correspond to the cellulose. These results indicate that conventional reactive ink deposited on paper not only forms silver oxide on the paper but also the distribution of formed nanoparticles on the surface of the cellulose fibers is not uniform. In contrast, XRD spectra of silver patterns formed with PVP-modified reactive ink on Whatman No. 1 paper do not display the diffraction peak at 2θ = 34.29° ascribed to Ag_2O. Moreover, sharp diffraction peaks indicate the absence of peaks attributed to silver oxides. Finally, the intensities of the diffraction peaks at 2θ = 15°, 2θ = 16.5°, and 2θ = 22.4°, which are attributed to the cellulose, were greatly decreased, confirming the improved distribution of silver NPs on the surface of cellulose. The results confirmed that PVP is playing a key role in the stabilization of silver cations that yield a higher amount of conductive silver nanoparticles with improved distribution, however, a high amount of PVP ratios showed an insulating effect. The best ratio of silver reactive ink, PVP solution, and DI water was found to be 4 : 1 : 1, respectively.

3.2. Formation of silver NPs on HEC-modified Whatman No. 1 paper

Based on our hypothesis that the hydroxyl functions of cellulose are inducing the formation of silver oxide, we decided to modify the paper to reduce the interaction of the silver cations with the hydroxyl groups. In this context, HEC was a good candidate because of its ethyl ether functionality instead of the hydroxyl group, and additionally, HEC was reported to be a good binder and stabilizer.[25] Fig. S1(B) (ESI†) shows the FTIR spectrum of

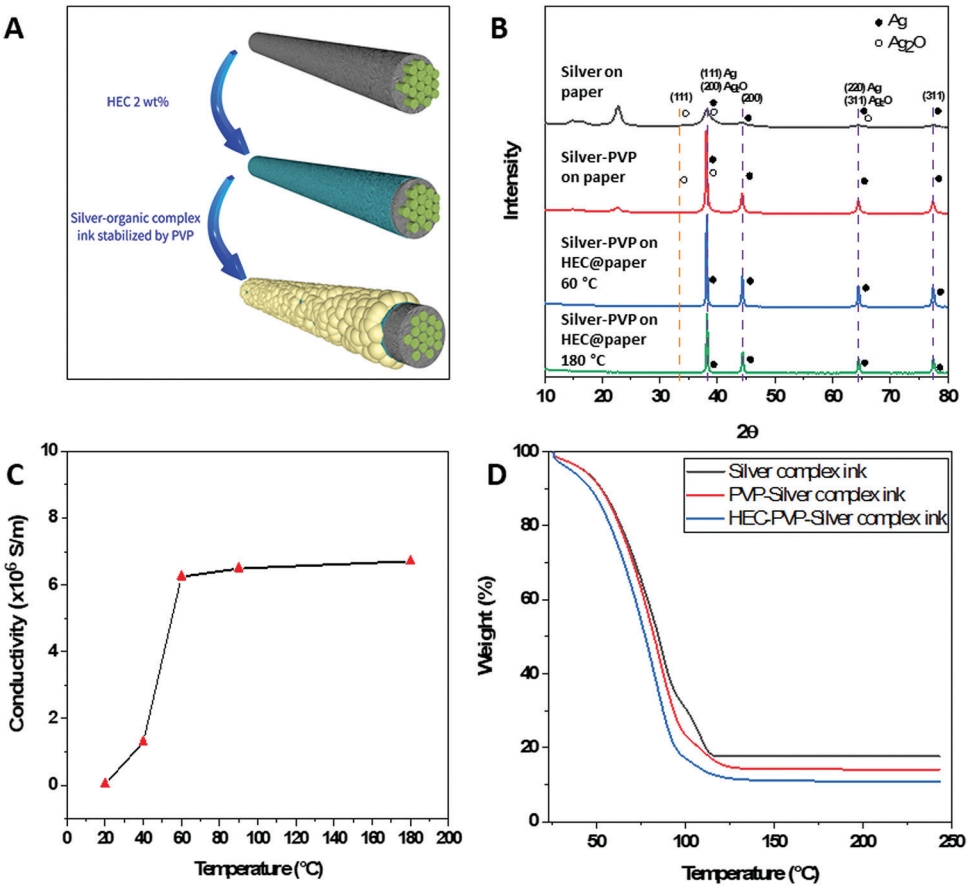

Fig. 1 Characterization of PVP stabilized silver complex ink. (A) Formation of silver nanoparticles on the surface of cellulose fiber. (B) XRD patterns of modified paper: silver-coated paper without PVP (black); PVP-stabilized silver coating on Whatman No. 1 paper (red); PVP-stabilized silver coating on HEC-modified Whatman No. 1 paper annealed at 60 °C (blue); PVP-stabilized silver coating on HEC-modified Whatman No. 1 paper annealed at 180 °C (green). (C) The electrical conductivity of PVP-stabilized Ag samples on HEC@Whatman No. 1 paper substrate annealed at different temperatures (D) TGA results of silver inks: silver-reactive ink (black); PVP-stabilized silver-reactive ink (red); PVP-stabilized silver-reactive ink mixed with HEC (blue).

silver patterns on HEC-modified Whatman No. 1 paper formed by the deposition of PVP-modified silver complex ink and annealing at 60 °C. The intensities of the resonance peak at 3162 cm^{-1} and 1050 cm^{-1} decreased, confirming the absence of silver oxide. Moreover, the decrease in intensity of characteristic peaks of cellulose paper indicates the full coverage of the cellulose fiber surface. The XRD patterns of silver complex ink modified by PVP deposited on HEC@Whatman No. 1 paper also do not display the diffraction peak attributed to silver oxide at $2\theta = 34.29°$, confirming the stabilizing effect of PVP (Fig. 1B). Additionally, the diffraction peaks at $2\theta = 15°$, $2\theta = 16.5°$, and $2\theta = 22.4°$, ascribed to the cellulose fibers, disappeared, confirming more uniform deposition of silver metal nanoparticles on the surface of the cellulose fibers, which is in accordance with the FTIR results. These results indicate that PVP plays a crucial role in stabilizing silver cations and prevents the formation of silver oxide, while HEC modification contributes to the formation of uniformly distributed silver nanoparticles on the surface of cellulose fibers.

Interestingly, modification of the Whatman No. 1 paper by HEC enabled the prepared patterns to be annealed at mild temperatures (60 °C). The XRD patterns of silver complex ink modified by PVP deposited on HEC@Whatman No. 1 paper annealed at 60 °C and 180 °C for 3 hours and 30 minutes, respectively, showing the same diffraction peaks corresponding to silver metal. To optimize the annealing temperatures silver patterns were incubated at different temperatures. The silver patterns annealed at 20 °C for 3 hours had a low conductivity of 3.45×10^4 S m^{-1}. By increasing the annealing temperature to 60 °C the conductivity of the patterns was improved to 6.246×10^6 S m^{-1}. Based on previously reported studies, in which the conductivity was improved by exposure to heat at high temperatures, we also checked the conductivity after annealing the patterns at 180 °C. Taking into consideration the sensitivity of the paper substrate to high temperatures we decreased the annealing time from 3 hours to 30 minutes. However, after annealing at 180 °C, the conductivity did not change much, indicating that silver cations generated from reactive ink were fully reduced in silver nanoparticles at 60 °C; therefore, annealing at 60 °C was found to be ideal. To study the effect of temperature on the formation of the silver metal nanoparticles we subjected the solution inks to thermo-gravimetric analysis (TGA), shown in Fig. 1(D). The TGA results of the unmodified silver complex ink revealed that the evaporation of ammonia and water is

responsible for the loss of 66 wt% mass in the range from 25 °C to 95 °C. The presence of a protracted plateau in the range 95–116 °C indicates the presence of residual silver acetate, which also explains the broad peak present on the XRD patterns.[11] Diaminesilver(I) complexes can exist only in solution and upon drying unreduced silver cations revert to salt form. The addition of PVP increases the rate of mass loss and results in the disappearance of the protracted plateau in the range 95–116 °C owing to the stabilization of the formed silver cations, which are subsequently reduced to silver metal. To study the effect of HEC on the stabilization of silver cations we have added 2 wt% HEC solution to the PVP-modified silver-reactive ink and TGA analysis was performed. As we can observe in Fig. 1(D) the rate of mass loss is increased and a protracted plateau in the range 95–116 °C disappeared. These results confirm the effect of HEC on the reduction of silver ions into silver metal nanoparticles at lower temperatures. These results confirm that HEC acts as a stabilizing and reducing agent of silver cations during the decomposition of AgR-ink.[26]

An important advantage of our developed method is the uniform distribution of conductive silver nanoparticles on the surface of the cellulose fibers. The FE-SEM images once again confirmed the uniform distribution of nanoparticles on the surface of the cellulose fiber (Fig. 2). As shown in Fig. 2(a and b), it is clear that Whatman paper on which silver complex ink has been deposited followed by annealing at 180 °C for 30 minutes tends to form aggregated nanoparticles on the surface of the fibers, which could also explain the absence of conductivity of the silver patterns prepared by this method. In contrast, the ink modified by PVP after annealing at 180 °C for 30 minutes showed superior uniformity, which also explains the increased conductivity, as shown in Fig. 2c and d. Finally, silver complex ink modified by PVP and deposited on HEC-modified Whatman paper has excellent uniformity at annealing temperatures of both 60 °C and 180°, as shown in the FE-SEM images in Fig. 2e–h.

3.3. Conductivity and porosity of silver patterned paper

In previously reported works, silver-reactive inks were deposited particularly on a substrate with low permeability and low surface roughness, such as PET, glass, and tracing paper which allows the accumulation of NPs on the surface of the substrate without penetrating the interior, resulting in the formation of a thin metallic layer with high conductivity on the surface of the substrate. Whereas the deposition of conductive silver patterns on macroporous Whatman No. 1 chromatography paper was achieved through the printing of commercially available silver NP colloidal ink.[27] This method allowed the porosity of macroporous paper to be preserved but resulted in low conductivity with the resistance measured to be in the range of 1 Ω to 10 Ω. From FE-SEM images we identified that the developed method enables the deposition of silver nanoparticles on the surface of cellulose fibers simultaneously preserving the porosity of microporous paper, see Fig. S2 (ESI†). Therefore, the two-probe resistance method and the thickness of the paper were used to calculate the conductivity of the silver patterns deposited using silver-reactive ink modified with PVP on HEC@Whatman paper (Fig. S2, ESI†). The conductivity of silver tracks was calculated to be 6.246×10^6 S m^{-1}. Resistances of silver tracks deposited on Whatman No. 1 paper *via* three different methods are presented in the ESI† (Fig. S3). The one-layer deposition of conventional silver reactive ink on microporous paper resulted in black colored patterns with no conductivity. However, the application of several layers of ink resulted in the formation of nanoparticles with very low conductivity. In contrast, the deposition of one layer of silver reactive ink modified with PVP showed relatively better conductivity with the resistance measured to be 31.6 Ω. Finally, the deposition of silver reactive

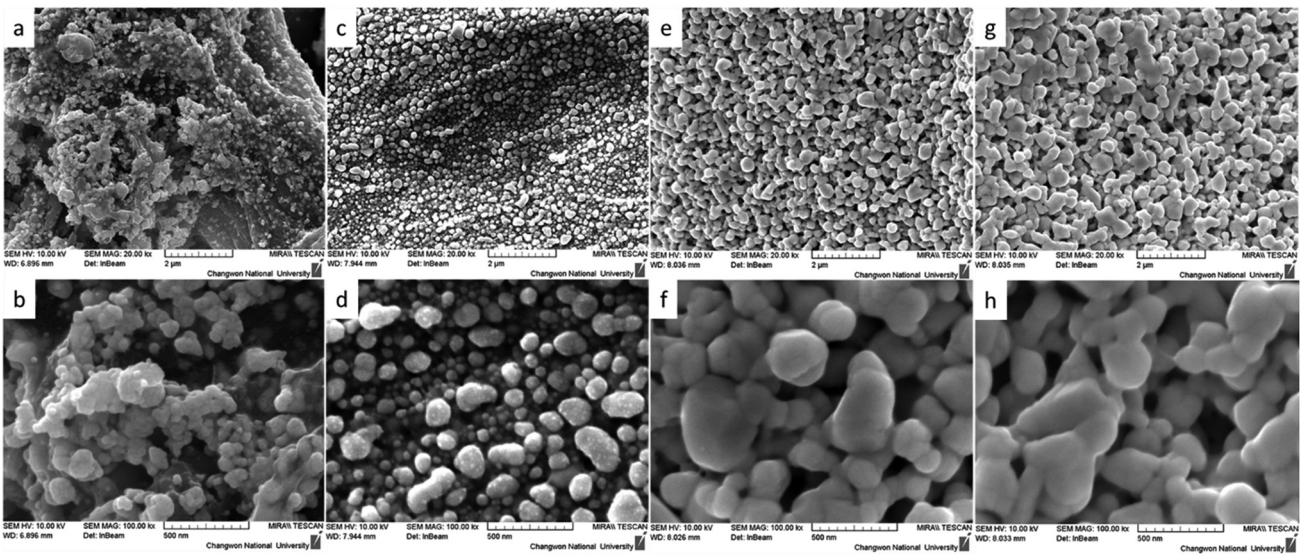

Fig. 2 FE-SEM images of modified papers. Silver-coated paper without PVP sintered at 180 °C (a and b). The PVP-stabilized silver coating on Whatman No. 1 paper annealed at 180 °C (c and d). The PVP-stabilized silver coating on HEC-modified Whatman No. 1 paper annealed at 60 °C (e and f). The PVP-stabilized silver coating on HEC-modified Whatman No. 1 paper annealed at 180 °C (g and h).

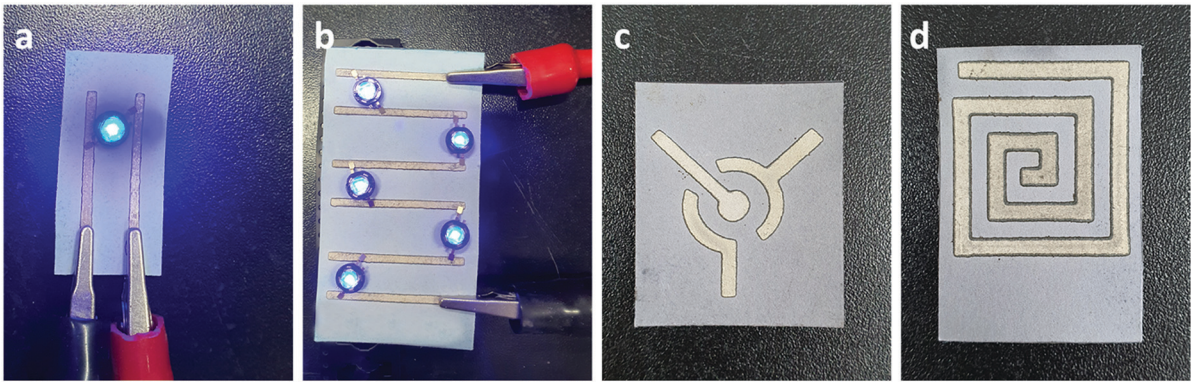

Fig. 3 Photographic images of applications of silver patterns on Whatman No. 1 paper. Paper-based flexible electronics (a and b). Paper-based electrodes for electrochemical sensing (c). Paper-based NFC patterns (d).

ink modified by PVP on HEC modified paper allowed a very high conductivity to be achieved with the resistance measured to be 0.4 Ω. The resistance of silver patterns deposited on microporous paper through a novel method was significantly lower owing to the uniform deposition of silver metal nanoparticles on the surface of cellulose fibers making them a promising candidate for electrofluidic applications. However, depending on the application the choice of paper may vary. Therefore, the formation of silver nanoparticles by deposition of PVP-modified silver-reactive ink on different paper substrates was investigated (Fig. S4, ESI†). Substrates with lower permeabilities showed a higher conductivity due to the accumulation of silver nanoparticles on the surface of the substrate. Sulfuric paper with very low permeability allowed accumulation of silver reactive ink on the surface thus resulting in the formation of a metallic layer on the surface of the sulfuric paper. To further investigate the porosity of silver patterns the wicking properties were investigated *via* the capillary rise method of rhodamine solution (10^{-3} M). As shown in Fig. S5 (ESI†) the immersion of 1.5 mm of silver patterns in rhodamine solution resulted in a migration of solution to about 7 mm through capillary pores. Although the aqueous solution was able to penetrate and migrate through silver-patterned paper, the migration rate was lower compared to non-patterned paper, on which aqueous solution has migrated to 12 mm during the identical time.

The high conductivity of silver patterns deposited by novel developed ink is suitable in the development of paper-based flexible electronics, to design paper-based electrochemical sensors, and to print radio-frequency identification (RFID) antennas (Fig. 3).

3.4. Electrowetting properties

3.4.1. Electrowetting properties of silver paper. To take full advantage of the novel approach, low voltage electrowetting properties of developed silver patterns and silver patterns-coated with ferroelectric polymers were investigated. Firstly, we investigated the penetration rate of aqueous solution through silver-patterned paper *versus* deposited silver ink volume and its electrowetting properties. Therefore, three different volumes of silver ink (60 μL, 30 μL, and 10 μL) were drop-casted on Whatman No. 1 paper substrate, and the penetration rate of 20 μL aqueous solution at different voltages was investigated (Fig. 4A). In the absence of voltage, the aqueous solution took 70 minutes to fully disappear from the surface of the paper patterned with 60 μL of silver ink. However, a small amount of stain on the absorbent pad located on the other side indicates that instead of penetration, evaporation took place. Although Whatman No. 1 paper patterned with silver nanoparticles preserve the porosity, the penetration rate of the aqueous solution is lowered due to the lotus effect[28] and high content of silver nanoparticles that clog the pores. Applying a voltage of 5 V and higher resulted in a decrease in penetration time on average to 35 minutes. The increased penetration rate of aqueous solution through silver patterns is enabled by the electrowetting properties of silver-coated cellulose fibers. These results are in accordance with results reported in previous research work that investigated the electrowetting properties of biocompatible/biodegradable cellulose and cellulose derivative dielectric material.[29] On the other hand, paper patterned with 30 μL silver ink showed faster penetration of an aqueous solution through a silver pattern. A decrease in silver ink volume resulted in lower silver content and reduced the pore filling. In the absence of voltage, the aqueous solution has fully penetrated in 16 minutes, while the application of voltage 5 V or higher decreased the penetration time to 10 minutes. The standard deviation of penetration time of silver patterned paper was found to be around 3 minutes for the flow of aqueous liquid while a low voltage up to 4 V was applied. This phenomenon can be explained by the uneven distribution of pores of the Whatman No. 1 paper. By increasing the voltage to 5 V, we observed a lower standard deviation. To further investigate the effect of silver content on flow rate, we have prepared silver patterns by drop-casting 10 μL silver ink on wax patterned disk-shaped paper. The conductivity of paper prepared with 10 μL silver ink was lower because of low silver content and non-uniform coating of cellulose fibers by silver nanoparticles. We further analyzed the penetration time of 20 μL aqueous solution by applying a voltage ranging from 0 to 12 V. Compared to silver patterns with higher silver content, these patterns showed a faster penetration rate due

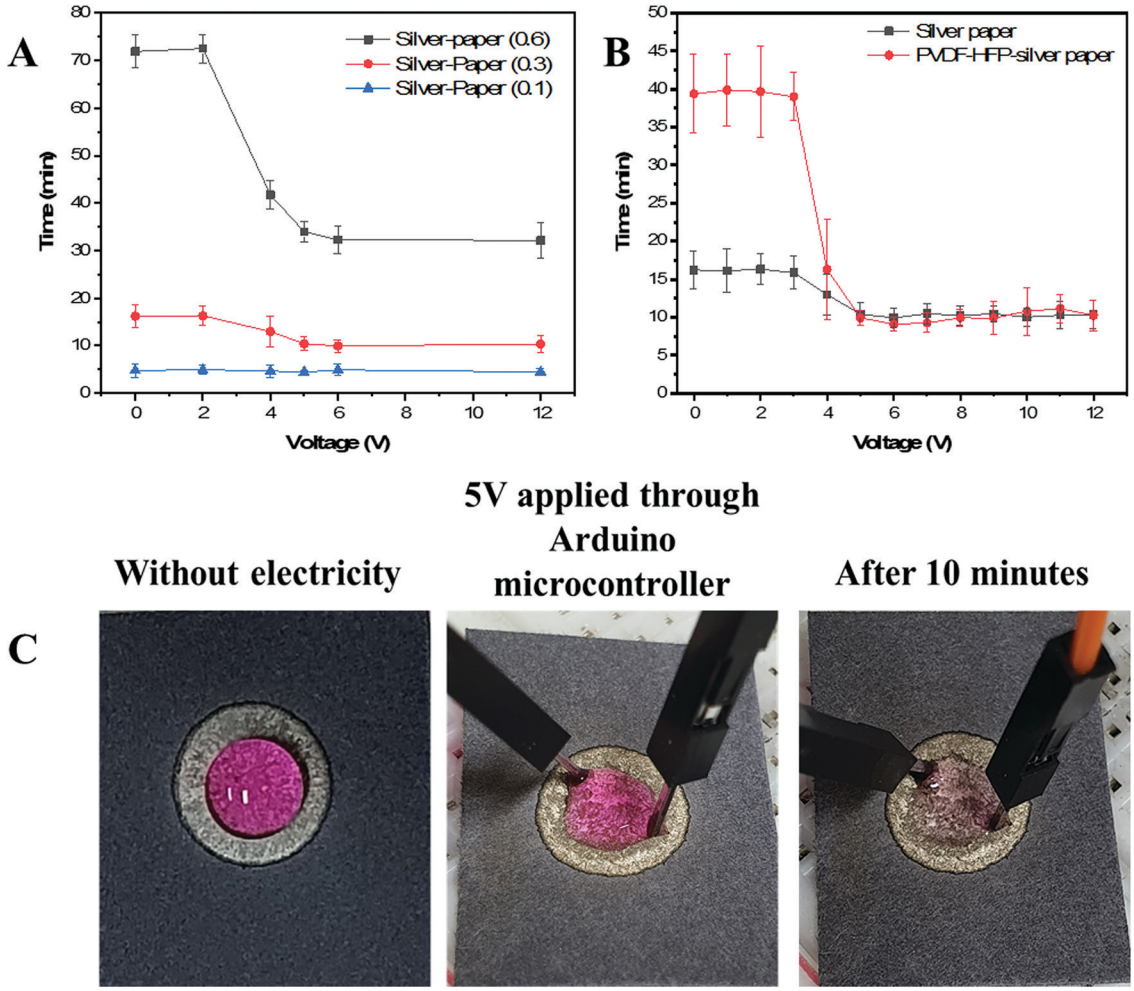

Fig. 4 Electrowetting properties of silver patterns and silver patterns coated PVDF-HFP films. Full penetration time of 20 μL aqueous solution *versus* voltage on silver patterned Whatman No. 1 paper with different silver volumes (A), full penetration time of 20 μL aqueous solution *versus* voltage on PVDF-HFP film-coated silver patterns on Whatman No. 1 paper (B), Photographic images of 20 μL aqueous solution in absence and presence of voltage. Rhodamine B was used for visualization purposes.

to the non-uniform deposition of silver nanoparticles on cellulose fibers and week lotus effect. The complete penetration of 20 μL aqueous solution through the paper with low content of silver nanoparticles was achieved within 4 minutes without applying a voltage. Interestingly, the application of voltage up to 12 V did not show any changes in wetting properties, which explains once again the non-uniform deposition of silver nanoparticles on cellulose fibers and lower conductivity of silver patterns.

3.4.2. Coating of silver paper with PVDF-HFP film. To further ameliorate the electrowetting properties, silver patterns prepared with 30 μL silver-reactive ink were coated by ferroelectric fluoropolymer: PVDF-HFP to transform them into the electrical valve. The PVDF-HFP is a hydrophobic fluorinated polymer[30] that has been successfully applied in electrowetting applications.[31] To form a uniform and thin layer film two different approaches were investigated. First, silver patterns were dip-coated in a PVDF-HFP solution and dried in a vacuum oven at 60 °C for 30 minutes. The dip-coating approach has shown good performance in the deposition of the ferroelectric film on the glass–ITO substrate,[31] however, in the case of wax patterned paper, this method was not appropriate because of the instability of wax patterns in organic solvents. On the other hand, the drop-casting method minimizes the contact of PVDF-HFP solutions with wax patterns thus preserving the intact wax barriers. To form a thin and uniform film various volumes of PVDF-HFP solutions (10 μL to 200 μL) were drop-casted on silver patterned paper and dried in the oven at 60 °C for 30 minutes (Fig. 5). The naked eye observation showed that drop-casting 10 μL of PVDF-HFP solution on silver paper disk with radius 5 mm allowed the formation of a film that was mostly distributed at the center of the disc, while the extremity of the disc was not covered well by the film (Fig. 5A). Therefore, the contact angle of the aqueous solution with silver patterns was different at a different location on the disc. As shown in Fig. 4A, the contact angle of the aqueous solution at the center of the silver pattern is higher compared to the contact angle at the extremity. Drop casting a higher volume of PVDF-HFP

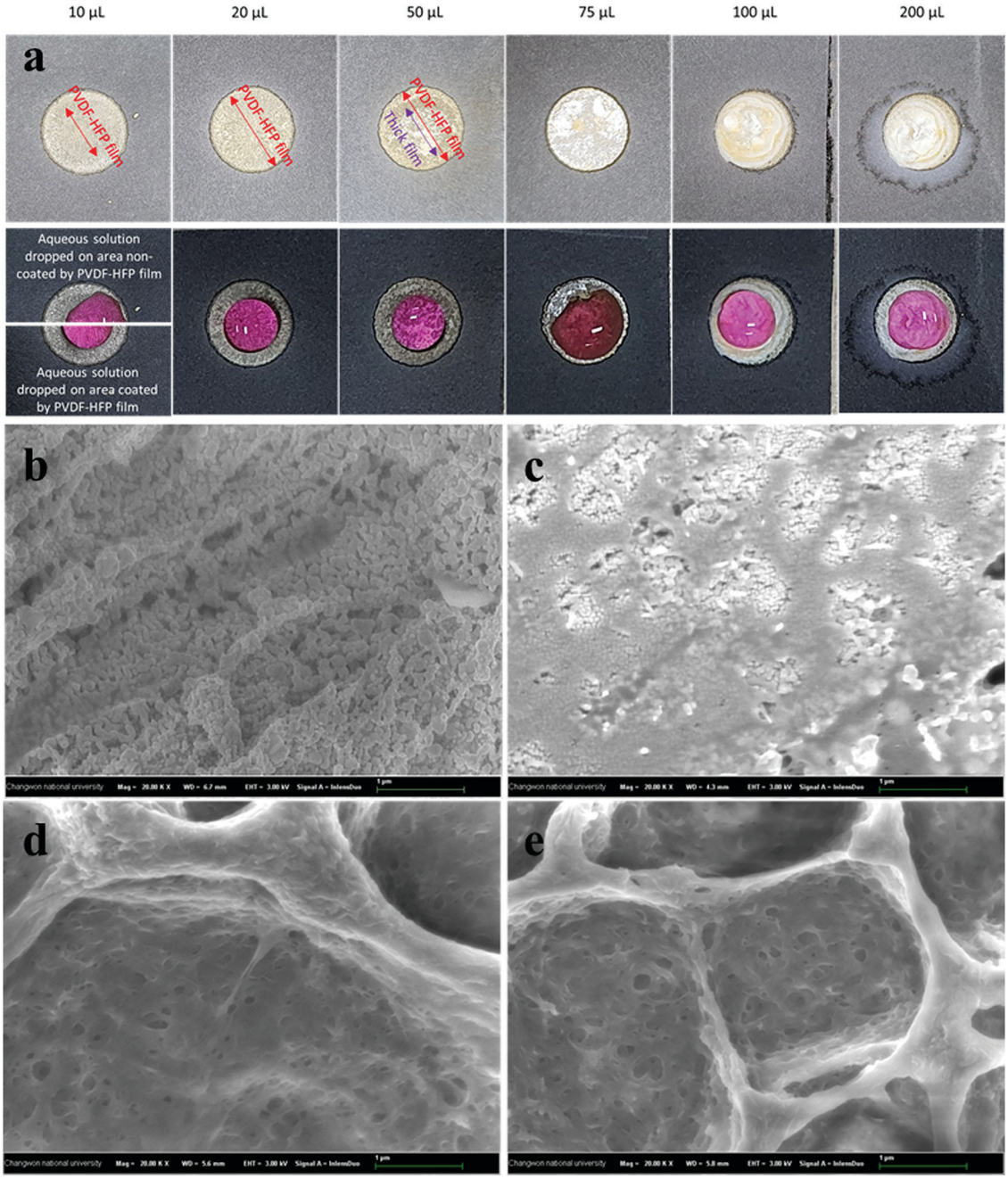

Fig. 5 Photographs and FE-SEM images of PVDF-HFP film-coated on silver patterns *via* drop-casting the different volumes of a polymer solution. Photographs of silver patterns coated with PVDF-HFP films and the surface tension with 20 μL aqueous solution (a). Silver-coated Whatman No. 1 paper (b). PVDF-HFP (20 μL) film on silver-coated Whatman No. 1 paper (c). PVDF-HFP (75 μL) film on silver-coated Whatman No. 1 paper(d). PVDF-HFP (200 μL) film on silver-coated Whatman No. 1 paper(e). Rhodamine B was used for visualization purposes.

solution (20 μL) resulted in uniform distribution of thin-film through the entire surface of the silver patterns thus allowing the same contact angle at different locations. Increasing the volume of drop-casted PVDF-HFP solution higher than 20 μL allowed the formation of less uniform and thicker films. For instance, PVDF-HFP film formed by drop-casting 50 μL of the solution is fully distributed on the surface of silver patterns but the central part of the film is thicker than the extremity region. By increasing the volume of PVDF-HFP solution to 75 μL we were able to form a thicker but still non-uniform film. The drop-casting PVDF-HFP solution whose volume exceeds 100 μL showed the penetration of the solution into the wax area. The PVDF-HFP coated silver tracks were further examined by low voltage FE-SEM techniques. As shown in Fig. 5B, the FE-SEM image of the silver track on Whatman No. 1 paper confirmed once again that developed ink allows the deposition of metallic

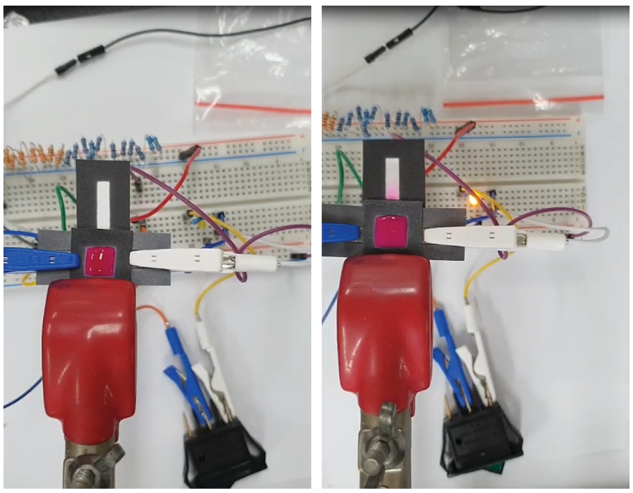

Fig. 6 Photographs of electro-responsive valves assembled in stacked system. The flow of rhodamine solution through electro-responsive valves in absence of voltage (left) and in presence of voltage 12 V (right) in 6 minutes. Rhodamine B was used for visualization purposes.

silver nanoparticles exclusively on the surface of cellulose fibers, simultaneously preserving the porosity of paper. The FE-SEM images of silver patterns coated with PVDF-HFP film confirmed that 20 μL is sufficient to form a thin film layer, while the volume of PVDF-HFP solution exceeding 75 μL induces the formation of a thicker film with a strongly manifested honeycomb shape.

3.4.3. Electrowetting properties of PVDF-HFP-silver paper. Deposition of PVDF-HFP film on silver patterns renders them more hydrophobic as a result decreasing the penetration rate of the aqueous solution, as shown in Fig. 4B. In the absence or at voltages up to 3 V, the full penetration time of 20 μL aqueous solution varies from 35 minutes to 45 minutes. The increased standard deviation at low voltages after coating the silver paper by PVDF-HFP results from the honeycomb-like structure of the PVDF-HFP film (Fig. 5c). However, in the presence of a voltage 5 V of higher the penetration time decreased to approximately 10 minutes with low standard deviations. The faster penetration rate of 20 μL aqueous solution at higher voltage is possible due to the changes in hydrophobicity of PVFD-HFP.

3.4.4. Electro-responsive valve integrated stacked microfluidic device. To investigate the practical application of electro-responsive valves developed by patterning paper with highly conductive silver nanoparticles-coated with PVDF-HFP, we have designed a stacked system (Fig. 6 and Video S1, ESI†). In the absence of an electric field, valves do not allow the penetration of an aqueous solution due to the hydrophobicity of PVDF-HFP and the lotus effect of silver nanoparticles. Our investigations showed that the electrowetting properties of cellulose and PVDF-HFP film enable penetration of aqueous solution in the presence of a voltage of 5 V and higher (Fig. 4B). Therefore, we have mounted a system that provides 12 V and connected it to the electro-responsive valve integrated stacked microfluidic device. As shown in Fig. 6 and Video S1 (ESI†), in the absence of voltage, the aqueous solution does not penetrate through the valve even with longer times. However, after the application of 12 V voltage, the aqueous solution starts to penetrate due to the electrowetting properties of PVDF-HFP-coated silver patterns.

3. Conclusion

In conclusion, we developed a novel formulation of silver-reactive ink modified by PVP that allows the stabilization of formed silver cations during the decomposition of complex, resulting in uniform deposition of conductive silver nanoparticles onto HEC-modified Whatman No. 1 paper. We used FTIR and XRD analysis techniques to confirm that the combination of PVP and HEC play an essential role in the stabilization of silver cations during their reduction to silver metal on microporous paper substrate. TGA results showed that PVP disables the reversion of unreduced silver cations into silver salt by stabilizing them while HEC decreases the annealing temperature of the silver complex ink to mild temperatures owing to their stabilizing effect. Finally, FE-SEM images confirmed the uniform deposition of metallic silver nanoparticles exclusively on the surface of cellulose fibers, which allow overcoming limitations encountered in the field of paper-based electronic devices, such as deposition of the conductive pattern on the surface of a substrate or to fill up the pores that limit the effective area and the possibility to design microfluidic devices.[10] To further exploit the developed method, we coated silver patterns with PVDF-HFP films and applied them as an electrical valve for a microfluidic device. Owing to the porosity of the silver patterns and the dielectric properties of cellulose and PVDF-HFP we were able to control the penetration rate of an aqueous solution by electrical stimulation.

Conflicts of interest

There are no conflicts to declare.

Acknowledgements

This work was supported by the Basic Science Research Program (NRF-2018R1A2B6001489 and NRF-2020R1A2C2007028) through the National Research Foundation of Korea.

References

1 M. Singh, H. M. Haverinen, P. Dhagat and G. E. Jabbour, *Adv. Mater.*, 2010, **22**, 673–685.
2 C. N. Hoth, S. A. Choulis, P. Schilinsky and C. J. Brabec, *Adv. Mater.*, 2007, **19**, 3973–3978.
3 P. Yang, L. Zhang, D. J. Kang, R. Strahl and T. Kraus, *Adv. Opt. Mater.*, 2020, **8**, 1901429.
4 S. Chung, K. Cho and T. Lee, *Adv. Sci.*, 2019, **6**, 1801445.
5 Y. Wang, C. Yan, S.-Y. Cheng, Z.-Q. Xu, X. Sun, Y.-H. Xu, J.-J. Chen, Z. Jiang, K. Liang and Z.-S. Feng, *Adv. Funct. Mater.*, 2019, **29**, 1902579.
6 B. Krykpayev, M. F. Farooqui, R. M. Bilal, M. Vaseem and A. Shamim, *Microelectron. J.*, 2017, **65**, 40–48.
7 Y. Wang, C. Zhu, R. Pfattner, H. Yan, L. Jin, S. Chen, F. Molina-Lopez, F. Lissel, J. Liu, N. I. Rabiah, Z. Chen,

J. W. Chung, C. Linder, M. F. Toney, B. Murmann and Z. Bao, *Sci. Adv.*, 2017, **3**, e1602076.
8 M. Santhiago, C. C. Corrêa, J. S. Bernardes, M. P. Pereira, L. J. M. Oliveira, M. Strauss and C. C. B. Bufon, *ACS Appl. Mater. Interfaces*, 2017, **9**, 24365–24372.
9 L. Huang, Y. Huang, J. Liang, X. Wan and Y. Chen, *Nano Res.*, 2011, **4**, 675–684.
10 M. M. Hamedi, A. Ainla, F. Güder, D. C. Christodouleas, M. T. Fernández-Abedul and G. M. Whitesides, *Adv. Mater.*, 2016, **28**, 5054–5063.
11 S. B. Walker and J. A. Lewis, *J. Am. Chem. Soc.*, 2012, **134**, 1419–1421.
12 W. Shen, X. Zhang, Q. Huang, Q. Xu and W. Song, *Nanoscale*, 2014, **6**, 1622–1628.
13 L. Mo, D. Liu, W. Li, L. Li, L. Wang and X. Zhou, *Appl. Surf. Sci.*, 2011, **257**, 5746–5753.
14 T. H. J. van Osch, J. Perelaer, A. W. M. de Laat and U. S. Schubert, *Adv. Mater.*, 2008, **20**, 343–345.
15 J. Perelaer, C. E. Hendriks, A. W. M. de Laat and U. S. Schubert, *Nanotechnology*, 2009, **20**, 165303.
16 C. E. Knapp, J.-B. Chemin, S. P. Douglas, D. A. Ondo, J. Guillot, P. Choquet and N. D. Boscher, *Adv. Mater. Technol.*, 2018, **3**, 1700326.
17 Q. Lei, J. He, B. Zhang, J. Chang and D. Li, *J. Mater. Chem. C*, 2018, **6**, 213–218.
18 W.-d. Yang, C.-y. Liu, Z.-y. Zhang, Y. Liu and S.-d. Nie, *J. Mater. Chem.*, 2012, **22**, 23012–23016.
19 Y. Jiang, Z. Hao, Q. He and H. Chen, *RSC Adv.*, 2016, **6**, 2888–2894.
20 C. K. W. Koo, F. He and S. R. Nugen, *Analyst*, 2013, **138**, 4998–5004.
21 L. Cai, M. Zhong, H. Li, C. Xu and B. Yuan, *Biomicrofluidics*, 2015, **9**, 046503.
22 B. Lutz, T. Liang, E. Fu, S. Ramachandran, P. Kauffman and P. Yager, *Lab Chip*, 2013, **13**, 2840–2847.
23 T. Guo, T. Meng, W. Li, J. Qin, Z. Tong, Q. Zhang and X. Li, *Nanotechnology*, 2014, **25**, 125301.
24 H. Wang, X. Qiao, J. Chen, X. Wang and S. Ding, *Mater. Chem. Phys.*, 2005, **94**, 449–453.
25 T. G. Majewicz, P. E. Erazo-Majewicz and T. J. Podlas, *Encyclopedia of Polymer Science and Technology*, Wiley-Interscience, 2002, DOI: 10.1002/0471440264.pst044.
26 M. A. El-Sheikh, S. M. El-Rafie, E. S. Abdel-Halim and M. H. El-Rafie, *J. Polym.*, 2013, 650837.
27 C. Gaspar, T. Sikanen, S. Franssila and V. Jokinen, *Biomicrofluidics*, 2016, **10**, 064120.
28 K. Ramaratnam, S. K. Iyer, M. K. Kinnan, G. Chumanov, P. J. Brown and I. Luzinov, *J. Eng. Fibers Fabr.*, 2008, **3**(4), DOI: 10.1177/155892500800300402.
29 L. Chao, Z. Zeng, K. Zhang, W. Wang and J. Zhou, *IEEE 11th International Conference on ASIC (ASICON)*, 2015, pp. 1–4.
30 W. Yang, F. Zhang, W. He, J. Liu, M. A. Hickner and B. E. Logan, *J. Power Sources*, 2014, **269**, 379–384.
31 Y. B. Sawane, S. B. Ogale and A. G. Banpurkar, *ACS Appl. Mater. Interfaces*, 2016, **8**, 24049–24056.